PHYSICAL REVIEW B **89**, 041101(R) (2014)

$CeIrIn_5$: Superconductivity on a magnetic instability

T. Shang,[1,2] R. E. Baumbach,[2] K. Gofryk,[2] F. Ronning,[2] Z. F. Weng,[1] J. L. Zhang,[1] X. Lu,[1] E. D. Bauer,[2] J. D. Thompson,[2] and H. Q. Yuan[1,*]

[1]*Center for Correlated Matter and Department of Physics, Zhejiang University, Hangzhou 310027, China*

[2]*Los Alamos National Laboratory, Los Alamos, New Mexico 87545, USA*

(Received 31 October 2013; published 3 January 2014)

We report on the doping-induced antiferromagnetic state and Fermi-liquid state that are connected by a superconducting region in a series of $CeIrIn_{5-x}Hg_x$, $CeIrIn_{5-x}Sn_x$, and $CeIr_{1-x}Pt_xIn_5$ single crystals. Measurements of the specific heat $C(T)$ and electrical resistivity $\rho(T)$ demonstrate that hole doping via Hg/In substitution gives rise to an antiferromagnetic ground state, but substitutions of In by Sn or Ir by Pt (electron doping) favor a paramagnetic Fermi-liquid state. A conelike non-Fermi-liquid region is observed near $CeIrIn_5$, showing a diverging effective mass on the slightly Hg-doped side. The obtained temperature-doping phase diagram suggests that $CeIrIn_5$ is in proximity to an antiferromagnetic quantum critical point, and heavy fermion superconductivity in this compound is mediated by magnetic quantum fluctuations rather than by valence fluctuations.

DOI: 10.1103/PhysRevB.89.041101 PACS number(s): 74.70.Tx, 74.40.Kb, 74.62.−c

The heavy fermion (HF) series $CeTIn_5$ (T = Co, Rh, Ir) has provided prototypical examples to study competing phases and their emergent behaviors arising from electron correlations.[1] $CeCoIn_5$ is a HF superconductor with the highest superconducting transition temperature ($T_{sc} = 2.3$ K) among the Ce-based HF compounds.[2] A slight substitution of In with Cd or Hg tunes the system to a long range antiferromagnetic (AFM) state.[3,4] Furthermore, application of pressure to the antiferromagnets $CeRhIn_5$ and $CeCo(In,Cd)_5$ eventually suppresses the AFM order and induces superconductivity (SC) near an AFM quantum critical point (QCP) (scenario I in Fig. 1).[4–7] The resulting superconducting phase diagram is nearly identical to that of $CeCoIn_5$ after a suitable pressure shift.[8] Thus, it has been widely accepted that $CeCoIn_5$ sits on the threshold of a magnetic instability at ambient pressure.[4–6,8–10]

$CeIrIn_5$, a sister compound of $CeCoIn_5$, shows similar HF SC without any coexisting magnetic order.[12] In spite of substantial efforts to understand the exotic properties in $CeIrIn_5$, the origin of its SC still remains controversial. Resembling that of $CeCu_2(Si,Ge)_2$,[13] a scenario of two superconducting domes was proposed for $CeIrIn_5$ under combined chemical and physical pressures (scenario II in Fig. 1).[14–16] $CeIrIn_5$ was argued to exist far from an AFM QCP and be located at a cusplike minimum of T_{sc}, which bridges the two superconducting domes.[16] Accordingly, superconductivity of $CeIrIn_5$ was proposed to be mediated by valence fluctuations rather than by spin fluctuations,[16–18] which are more commonly taken to mediate pairing in HF superconductors (scenario I in Fig. 1).[13,19] However, solid evidence of a valence instability has yet to be revealed in $CeIrIn_5$, even though nuclear quadrupolar resonance (NQR) experiments detected some differences between the two superconducting domes.[17,18] On the other hand, analyses of nuclear spin-lattice relaxation experiments indicated that the quantum critical behavior of $CeIrIn_5$ is more consistent with a spin-density-wave (SDW) scenario.[20] Moreover, measurements of thermal conductivity and penetration depth support a $d_{x^2-y^2}$-type gap symmetry in $CeIrIn_5$, the same as $CeCoIn_5$.[21–23] In order to examine the above two scenarios and, therefore, to unravel the nature of SC in $CeIrIn_5$, it is crucial to establish whether it is adjacent to a magnetic or a valence instability.

In this Rapid Communication, we tune the ground state of $CeIrIn_5$ by chemical substitutions on the Ir or In sites and characterize their physical properties by specific heat and electrical resistivity measurements. It is shown that $CeIrIn_5$ lies near an AFM QCP, where non-Fermi-liquid (NFL) behaviors and diverging effective mass are observed. Our results suggest that the SC of $CeIrIn_5$ is mediated by spin fluctuations, constraining a theoretical model for the origin of SC in $CeIrIn_5$.

Single crystals of $CeIrIn_{5-x}Hg_x$ ($0 \leqslant x_{Hg} \leqslant 0.225$), $CeIrIn_{5-x}Sn_x$ ($0 \leqslant x_{Sn} \leqslant 0.35$), and $CeIr_{1-x}Pt_xIn_5$ ($0 \leqslant x_{Pt} \leqslant 0.264$) were grown by an indium self-flux method. Room-temperature powder x-ray diffraction confirms that all the samples crystallize in the tetragonal $HoCoGa_5$ structure. The actual concentrations of Hg, Sn, and Pt were determined by microprobe analysis and single-crystal x-ray diffraction, and are 20%, 50%, and 44% of their nominal values, respectively. The actual concentrations rather than the nominal ones are used hereafter. Measurements of the electrical resistivity and specific heat were performed in a Quantum Design physical properties measurement system (PPMS-9T). The temperature dependence of the electrical resistivity was measured with a four-point method from 0.4 to 300 K by a LR700 resistance bridge combined with the PPMS temperature control system.

Figure 2 shows the temperature dependence of the specific heat C_e/T on a semilog scale for $CeIrIn_{5-x}Hg_x$, $CeIrIn_{5-x}Sn_x$, and $CeIr_{1-x}Pt_xIn_5$. The electronic contributions to the specific heat C_e are obtained by subtracting a phonon contribution, with the specific heat of $LaIrIn_5$ as a reference ($C_{LaIrIn_5}/T = \gamma + \beta T^2$, $\gamma \approx 5.8\,\mathrm{mJ/mol\,K^2}$, and $\beta \approx 1.25\,\mathrm{mJ/mol\,K^4}$). The specific heat of pure $CeIrIn_5$ was taken from Ref. 24, which follows NFL behavior above 1 K, i.e., $C_e/T \sim -\log T$. At lower temperatures, C_e/T tends to be a constant, which may reflect a possible Landau Fermi-liquid (FL) state. The sharp jump at $T_{sc} = 0.4$ K marks the bulk SC. Upon Hg substitution, bulk superconductivity is suppressed to lower temperatures

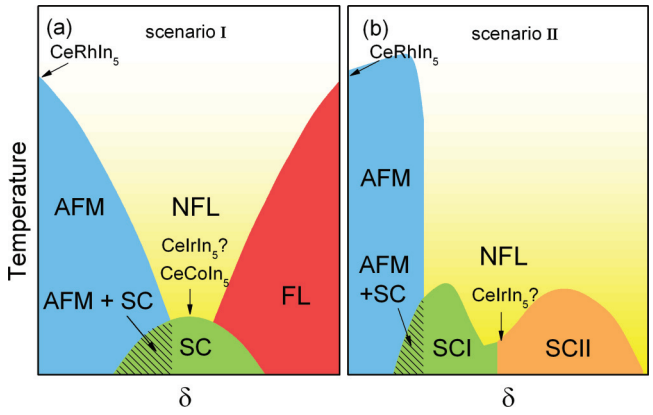

FIG. 1. (Color online) Schematic diagrams of two different scenarios for HF superconductors. Here δ represents a tuning parameter, such as pressure or doping. (a) Scenario I: A superconducting dome appears upon suppressing the AFM transition to a QCP (Ref. 11), which applies to most Ce-based HF superconductors including $CeCoIn_5$ and $CeRhIn_5$ (Refs. 4–8). (b) Scenario II: Two superconducting domes (SC I and SC II) develop upon increasing the lattice density (Ref. 13). SC I corresponds to scenario I, where SC is formed via critical spin fluctuations, and SC II shows a superconducting state presumably arising from valence fluctuations (Ref. 19).

(below 0.38 K). For $x_{Hg} = 0.027$, a logarithmic temperature dependence of C_e/T extends to lower temperatures. With further increasing the Hg concentration, a kink appears at 1.3 and 1.7 K for $x_{Hg} = 0.045$ and 0.054, respectively. Similar anomalies have been reported previously in $CeCo(In,Cd)_5$ and $CuCu_2Si_2$,[4,25] which are attributed to an AFM transition. After subtracting a logarithmic contribution of the spin fluctuations near a QCP, a pronounced transition is resolved in the specific heat $\Delta C_e/T$ for $x_{Hg} = 0.045$ and 0.054 [see the upper inset of Fig. 2(a)]. With this method, we clearly track the evolution of the Néel temperature T_N as a function of Hg content down to very low doping. Upon applying a magnetic field, the magnetic transition is eventually suppressed. As an example, we plot the specific heat $C_e(T)/T$ of $x_{Hg} = 0.054$ and 0.225 at two different magnetic fields in the lower inset of Fig. 2(a). For $x_{Hg} = 0.054$, the specific heat C_e/T demonstrates a logarithmic temperature dependence down to the lowest temperatures as the magnetic order is suppressed at 7 T. It is worth noting that the plateau below 1 K in pure $CeIrIn_5$ is very robust against an external magnetic field[26] and is different from the magnetic anomalies shown in $x_{Hg} = 0.045$ and 0.054. The extension of the NFL behavior and the absence of magnetic order for $x_{Hg} = 0.027$ indicates that an AFM QCP lies in proximity to this Hg content. With further increasing x_{Hg} (>0.054), the specific heat C_e/T shows a pronounced AFM transition: T_N increases with increasing x_{Hg} and reaches $T_N = 8$ K at $x_{Hg} = 0.225$. The magnetic transition is robust against a magnetic field, as typically seen in heavy fermion antiferromagnets, e.g., in $CeRhIn_5$.[27]

In contrast to Hg substitution (hole doping), electron doping via Sn/In or Pt/Ir substitutions exhibits remarkably different behaviors. In Figs. 2(b) and 2(c), we plot the specific heat $C_e(T)/T$ for $CeIrIn_{5-x}Sn_x$ and $CeIr_{1-x}Pt_xIn_5$.

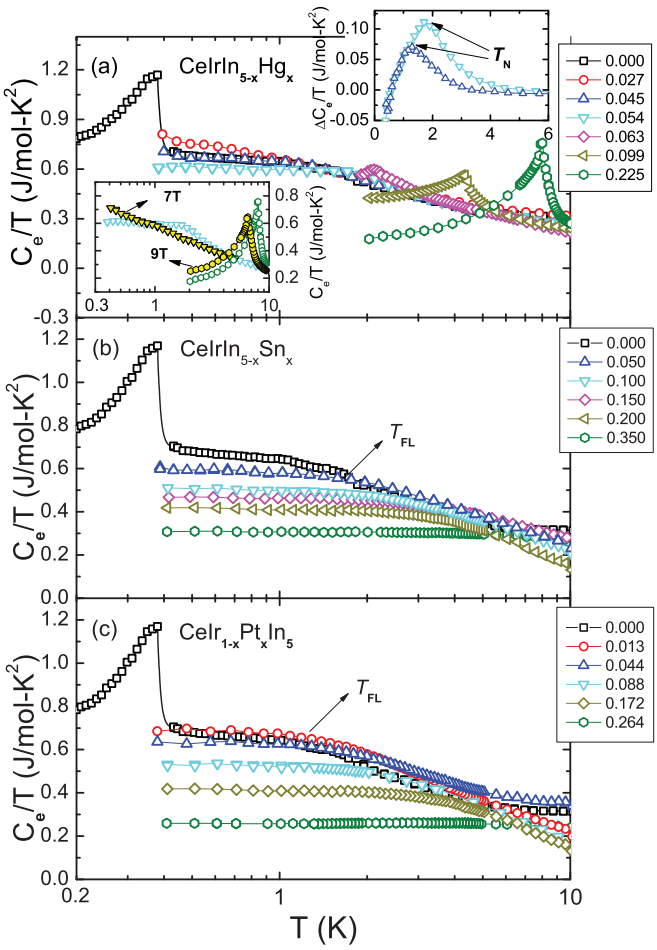

FIG. 2. (Color online) Temperature dependence of the specific heat for (a) $CeIrIn_{5-x}Hg_x$, (b) $CeIrIn_{5-x}Sn_x$, and (c) $CeIr_{1-x}Pt_xIn_5$. The upper inset plots the specific heat $\Delta C_e/T$ after subtracting a logarithmic contribution for $x_{Hg} = 0.045$ and 0.054. The lower inset plots the specific heat for $x_{Hg} = 0.054$ and 0.225 at a magnetic field of $B = 0$, 7 T ($x_{Hg} = 0.054$), and 9 T ($x_{Hg} = 0.225$), respectively. The magnetic field is orientated along the c axis.

These two series of compounds behave nearly identically, being independent of the dopant sites, similar to Sn- and Pt-doped $CeCoIn_5$.[3] A tiny amount of Sn or Pt dopants suppress the superconducting transition below $T = 0.38$ K in the specific heat. No evidence of magnetic order is observed in the electron-doped compounds. Instead, the specific heat C_e/T becomes constant at low temperatures, indicating a FL ground state. The FL temperature T_{FL}, which marks the onset temperature of the constant C_e/T, increases with increasing the electron dopants. On the other hand, the specific heat Sommerfeld coefficient γ, obtained by extrapolating C_e/T to zero temperature, monotonically decreases when increasing the Sn or Pt concentrations.

The above behaviors are further supported by measurements of transport properties. Figure 3 plots the electrical resistivity $\rho(T)$ of (a) $CeIr_{1-x}Hg_xIn_5$ and (b) $CeIrIn_{5-x}Sn_x$ at several representative doping concentrations. As already seen in the specific heat data, the resistivity of $CeIr_{1-x}Pt_xIn_5$ (not shown) gives nearly identical behaviors to that of

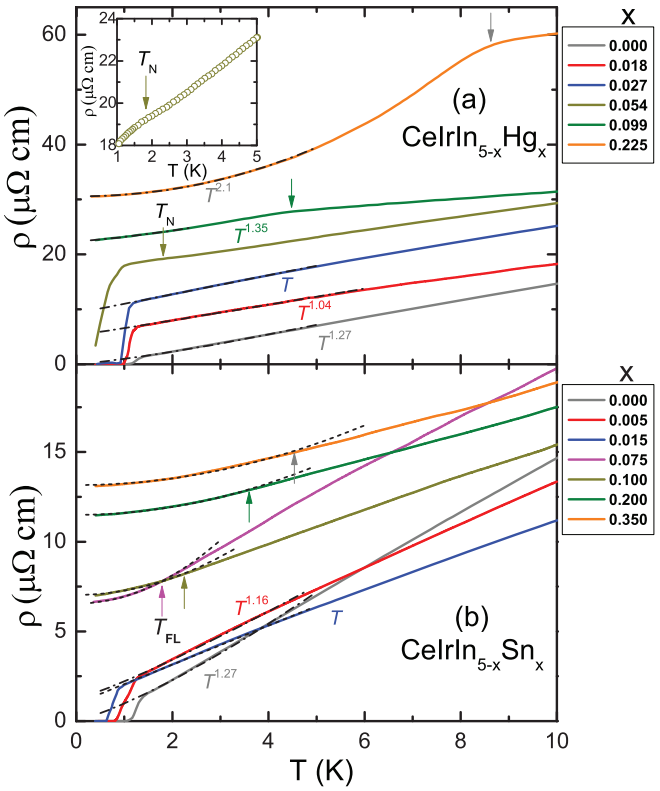

FIG. 3. (Color online) Temperature dependence of the electrical resistivity $\rho(T)$ for (a) $CeIr_{1-x}Hg_xIn_5$ and (b) $CeIrIn_{5-x}Sn_x$. The inset enlarges the electrical resistivity at low temperatures for $x_{Hg} = 0.054$, showing a resistive anomaly around $T_N \simeq 1.8$ K. The arrows mark the AFM transition in the top panel and the FL temperature T_{FL} in the bottom panel, respectively. The dashed lines show fits to $\rho = \rho_0 + AT^2$, and the dotted-dashed lines are fits to $\rho = \rho_0 + AT^n$. For $x_{Hg} = 0.099$ and 0.225, the electrical resistivity is fit to temperatures below 50% of T_N.

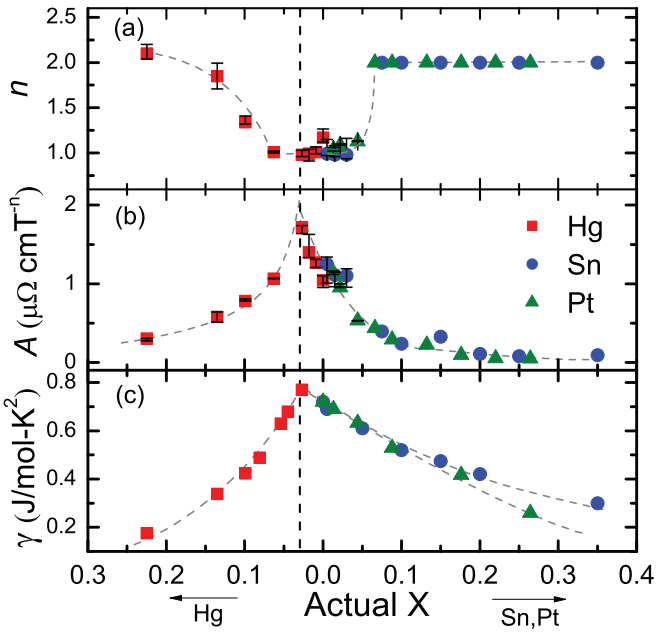

FIG. 4. (Color online) Doping dependence of (a) the resistive exponent n, (b) the A coefficient, and (c) the specific heat coefficient γ for $CeIrIn_{5-x}Hg_x$, $CeIrIn_{5-x}Sn_x$, and $CeIr_{1-x}Pt_xIn_5$ (to the left: Hg content; to the right: Sn or Pt content). The vertical dashed line marks the critical concentration at $x^c_{Hg} = 0.027$. The error bars are a result of changing fit ranges.

$CeIrIn_{5-x}Sn_x$. Superconductivity only shows up near stoichiometric $CeIrIn_5$, and is suppressed by substituting either a tiny amount of Hg on the In sites or Sn on the In sites. The resistive T_{sc} is higher than the corresponding bulk values from the specific heat, which was argued to result from the formation of a textured superconducting phase.[28] Furthermore, for those superconducting samples their normal-state resistivity follows a behavior of $\rho = \rho_0 + AT^n$ ($n < 1.3$) at low temperatures, as illustrated in Fig. 3 by the dotted-dashed lines, exhibiting a NFL behavior. The AFM transitions can be well tracked in the electrical resistivity $\rho(T)$ of Hg-doped samples ($x_{Hg} \geqslant 0.045$) [see the arrows in Fig. 3(a)], whose transition temperatures are highly consistent with those derived from the specific heat data. For a better illustration of the weak magnetic transition in the low-doping region, the resistivity of $x_{Hg} = 0.054$ at low temperatures is expanded in the inset, where a resistive kink marked by the arrow can be observed around $T_N \approx 1.8$ K. With increasing the Hg concentration, the magnetic transition becomes more pronounced and T_N shifts to higher temperatures. On the other hand, no evidence for a magnetic transition is found in the $CeIrIn_{5-x}Sn_x$ samples over the entire Sn-doping range. For $x_{Sn} \geqslant 0.075$, their low-temperature electrical resistivity can be well fitted by $\rho = \rho_0 + AT^2$ [see the dashed line in Fig. 3(b)], suggesting a FL ground state as seen in the specific heat data C_e/T. The FL temperature T_{FL}, above which the resistivity deviates from the quadratic temperature dependence, increases with increasing the Sn concentration. For all the doped compounds, the residual resistivity ρ_0 increases with the dopant concentration, which seems to be mainly caused by disorders introduced by elemental substitutions.

To extend the above analyses of electrical resistivity, we fit the low-temperature resistivity with a power-law expression $\rho = \rho_0 + AT^n$ for all the measured samples. In Fig. 4, the derived parameters of the resistive exponent n and the A coefficient, together with the Sommerfeld coefficient γ from the specific heat, are plotted as a function of the doping concentration for $CeIrIn_{5-x}Hg_x$, $CeIrIn_{5-x}Sn_x$, and $CeIr_{1-x}Pt_xIn_5$. For $x_{Hg} \geqslant 0.063$, we simply take the lowest-temperature value in $C_e(T)/T$ as γ. Slightly on the Hg-doped side as marked by the dashed line, both the resistive A coefficient and the specific heat coefficient γ demonstrate a diverging behavior around a critical value of $x^c_{Hg} = 0.027$. Furthermore, pronounced NFL behaviors with a linear-temperature dependence ($n \simeq 1$) of the electrical resistivity as well as a logarithmic-type temperature dependence in the specific heat $C_e(T)/T$ (see Fig. 2) are observed near this critical concentration. Away from $x^c_{Hg} = 0.027$, a FL ground state with $n = 2$ is quickly recovered. It is noted that within the magnetically ordered state the extra electron-magnon scattering increases the resistive exponent n beyond the FL prediction, e.g., $n = 2.1$ for $x_{Hg} = 0.225$.

In Fig. 5, we present a combined temperature-doping phase diagram for $CeIrIn_{5-x}Hg_x$, $CeIrIn_{5-x}Sn_x$, and $CeIr_{1-x}Pt_xIn_5$, constructed from the measurements of electrical resistivity

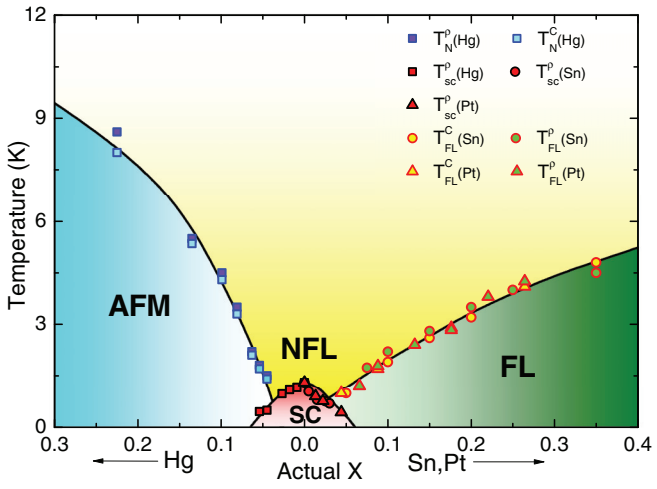

FIG. 5. (Color online) The magnetic and superconducting phase diagram of $CeIrIn_5$ as a function of Hg-, Sn-, and Pt-doping concentration. Different symbols represent different phase transitions (T_{sc} or T_N) or characteristic temperatures (T_{FL}). The different colors of the symbols mark different measurements of physical quantities used to determine the transition temperatures. Here the superconducting transition temperature T_{sc}^{ρ} is obtained by the midpoint of the resistive drop at T_{sc}.

and specific heat. The left horizontal axis stands for Hg concentration, while the right one is for Sn or Pt concentration. $CeIrIn_5$ exhibits a resistive superconducting transition at $T_{sc} = 1.2$ K, but a bulk transition at $T_{sc} = 0.4$ K in the specific heat. Upon partially substituting Hg with In (hole doping), the resistive SC is observed in a narrow doping range of $0.0 \leqslant x_{Hg} \leqslant 0.054$ at temperatures above $T = 0.38$ K, and AFM order eventually develops for $x_{Hg} \geqslant 0.045$, with T_N reaching 8 K at $x_{Hg} = 0.225$. Around the critical concentration of $x_{Hg}^c = 0.027$, both the specific heat $C_e(T)/T$ and the electrical resistivity $\rho(T)$ demonstrate NFL behaviors over a wide temperature range, which can be described in terms of the spin fluctuation theory with anisotropic scattering.[29] On the other side, SC survives for the Sn/In or Pt/Ir substitution (electron doping) in the region of $0.0 \leqslant x_{Sn} \leqslant 0.03$ ($0.0 \leqslant x_{Pt} \leqslant 0.044$). When increasing the dopant concentrations, a FL ground state is quickly recovered, as observed in both the electrical resistivity and the specific heat. The FL temperature T_{FL} monotonically increases with increasing the Sn or Pt concentrations. A wide conelike NFL region sits between the AFM and FL states on top of the SC dome. These results resemble those of Cd-doped $CeCoIn_5$ and pressurized $CePd_2Si_2$ and $CeRhIn_5$, as schematically illustrated in Fig. 1(a) for scenario I,[4–8,11] where SC emerges near an AFM QCP. Our results provide solid evidence that $CeIrIn_5$ is located near an AFM instability rather than a valence instability and the SC of $CeIrIn_5$ is associated with critical spin fluctuations, being similar to many other HF superconductors. We note that the strongest evidence for scenario II in $CeIrIn_5$ is due to the increase of T_{sc} in the pure compound under pressure.[17,18] However, a similar increase of T_{sc} under pressure is observed in pure $CeCoIn_5$ where spin-fluctuation-mediated SC is generally believed.[8] However, we cannot exclude the possibility that a degenerate valence instability may take place near the AFM QCP, as theoretically argued for $CeRhIn_5$.[30]

In summary, we have obtained a combined temperature-doping phase diagram for $CeIrIn_{5-x}Hg_x$, $CeIrIn_{5-x}Sn_x$, and $CeIr_{1-x}Pt_xIn_5$ based on a systematic study of their transport and thermodynamic properties. Upon substituting In with Hg in $CeIrIn_5$, AFM order develops at low temperatures. The system shows pronounced NFL behaviors over a wide temperature region near the critical concentration $x_{Hg}^c = 0.027$, where a superconducting dome is observed. Our results demonstrate that $CeIrIn_5$ lies in the vicinity of an AFM QCP and its SC is likely mediated by spin fluctuations rather than valence fluctuations. This is in line with the recent theoretical predictions,[31] and suggests a unified picture of SC in the $CeTIn_5$ family as well as many other HF superconductors.

This work is partially supported by the National Science Foundation of China (Grants No. 11174245, No. 10934005, and No. 11374257), the National Basic Research Program of China (973 Program) (2009CB929104, 2011CBA00103), Zhejiang Provincial Natural Science Foundation of China, and the Fundamental Research Funds for the Central Universities. Work at LANL was performed under the auspices of the Department of Energy, Office of Basic Energy Sciences, Division of Materials Science and Engineering.

*hqyuan@zju.edu.cn

[1] J. D. Thompson and Z. Fisk, J. Phys. Soc. Jpn. **81**, 011002 (2012).
[2] C. Petrovic, P. G. Pagliuso, M. F. Hundley, R. Movshovich, J. L. Sarrao, J. D. Thompson, Z. Fisk, and P. Monthoux, J. Phys.: Condens. Matter. **13**, L337 (2001).
[3] K. Gofryk, F. Ronning, J.-X. Zhu, M. N. Ou, P. H. Tobash, S. S. Stoyko, X. Lu, A. Mar, T. Park, E. D. Bauer, J. D. Thompson, and Z. Fisk, Phys. Rev. Lett. **109**, 186402 (2012).
[4] L. D. Pham, T. Park, S. Maquilon, J. D. Thompson, and Z. Fisk, Phys. Rev. Lett. **97**, 056404 (2006).
[5] E. D. Bauer, C. Capan, F. Ronning, R. Movshovich, J. D. Thompson, and J. L. Sarrao, Phys. Rev. Lett. **94**, 047001 (2005); S. M. Ramos, M. B. Fontes, E. N. Hering, M. A. Continentino, E. Baggio-Saitovich, F. D. Neto, E. M. Bittar, P. G. Pagliuso, E. D. Bauer, J. L. Sarrao, and J. D. Thompson, *ibid.* **105**, 126401 (2010).
[6] S. Zaum, K. Grube, R. Schäfer, E. D. Bauer, J. D. Thompson, and H. V. Löhneysen, Phys. Rev. Lett. **106**, 087003 (2011).
[7] T. Park, F. Ronning, H. Q. Yuan, M. B. Salamon, R. Movshovich, J. L. Sarrao, and J. D. Thompson, Nature (London) **440**, 65 (2006); G. Knebel, D. Aoki, D. Braithwaite, B. Salce, and J. Flouquet, Phys. Rev. B **74**, 020501(R) (2006).
[8] V. A. Sidorov, M. Nicklas, P. G. Pagliuso, J. L. Sarrao, Y. Bang, A. V. Balatsky, and J. D. Thompson, Phys. Rev. Lett. **89**, 157004 (2002).
[9] A. Bianchi, R. Movshovich, I. Vekhter, P. G. Pagliuso, and J. L. Sarrao, Phys. Rev. Lett. **91**, 257001 (2003).
[10] Y. Tokiwa, E. D. Bauer, and P. Gegenwart, Phys. Rev. Lett. **111**, 107003 (2013).
[11] N. D. Mathur, F. M. Grosche, S. R. Julian, I. R. Walker, D. M. Freye, R. K. W. Haselwimmer, and G. G. Lonzarich,

Nature (London) **394**, 39 (1998); P. Monthoux, D. Pines, and G. G. Lonzarich, *ibid.* **450**, 1177 (2007).

[12]C. Petrovic, R. Movshovich, M. Jaime, P. G. Pagliuso, M. F. Hundley, J. L. Sarrao, Z. Fisk, and J. D. Thompson, Europhys. Lett. **53**, 354 (2001).

[13]H. Q. Yuan, F. M. Grosche, M. Deppe, C. Geibel, G. Sparn, and F. Steglich, Science. **302**, 2104 (2003); H. Q. Yuan, F. M. Grosche, M. Deppe, G. Sparn, C. Geibel, and F. Steglich, Phys. Rev. Lett. **96**, 047008 (2006).

[14]P. G. Pagliuso, C. Petrovic, R. Movshovich, D. Hall, M. F. Hundley, J. L. Sarrao, J. D. Thompson, and Z. Fisk, Phys. Rev. B **64**, 100503 (2001).

[15]M. Nicklas, V. A. Sidorov, H. A. Borges, P. G. Pagliuso, J. L. Sarrao, and J. D. Thompson, Phys. Rev. B **70**, 020505(R) (2004).

[16]S. Kawasaki, M. Yashima, Y. Mugino, H. Mukuda, Y. Kitaoka, H. Shishido, and Y. Ōnuki, Phys. Rev. Lett. **96**, 147001 (2006).

[17]S. Kawasaki, G.-Q. Zheng, H. Kan, Y. Kitaoka, H. Shishido, and Y. Ōnuki, Phys. Rev. Lett. **94**, 037007 (2005).

[18]M. Yashima, N. Tagami, S. Taniguchi, T. Unemori, K. Uematsu, H. Mukuda, Y. Kitaoka, Y. Ōta, F. Honda, R. Settai, and Y. Ōnuki, Phys. Rev. Lett. **109**, 117001 (2012).

[19]K. Miyake, O. Narikiyo, and Y. Onishi, Physica B **259–261**, 676 (1999); Y. Onishi and K. Miyake, J. Phys. Soc. Jpn. **69**, 3955 (2000); A. T. Holmes, D. Jaccard, and K. Miyake, Phys. Rev. B **69**, 024508 (2004).

[20]S. Kambe, H. Sakai, Y. Tokunaga, and R. E. Walstedt, Phys. Rev. B **82**, 144503 (2010).

[21]Y. Kasahara, T. Iwasawa, Y. Shimizu, H. Shishido, T. Shibauchi, I. Vekhter, and Y. Matsuda, Phys. Rev. Lett. **100**, 207003 (2008).

[22]D. Vandervelde, H. Q. Yuan, Y. Ōnuki, and M. B. Salamon, Phys. Rev. B **79**, 212505 (2009).

[23]K. An, T. Sakakibara, R. Settai, Y. Onuki, M. Hiragi, M. Ichioka, and K. Machida, Phys. Rev. Lett. **104**, 037002 (2010).

[24]E. D. Bauer, F. Ronning, S. Maquilon, L. D. Pham, J. D. Thompson, and Z. Fisk, Physica B **403**, 1135 (2008).

[25]E. Lengyel, M. Nicklas, H. S. Jeevan, C. Geibel, and F. Steglich, Phys. Rev. Lett. **107**, 057001 (2011).

[26]C. Capan, A. Bianchi, F. Ronning, A. Lacerda, J. D. Thompson, M. F. Hundley, P. G. Pagliuso, J. L. Sarrao, and R. Movshovich, Phys. Rev. B **70**, 180502(R) (2004).

[27]L. Jiao, H. Q. Yuan, Y. Kohama, E. D. Bauer, J.-X. Zhu, J. Singleton, T. Shang, J. L. Zhang, Y. Chen, H. O. Lee, T. Park, M. Jaime, J. D. Thompson, F. Steglich, and Q. Si, arXiv:1308.0294.

[28]T. Park, H. O. Lee, I. Martin, X. Lu, V. A. Sidorov, K. Gofryk, F. Ronning, E. D. Bauer, and J. D. Thompson, Phys. Rev. Lett. **108**, 077003 (2012).

[29]J. A. Hertz, Phys. Rev. B **14**, 1165 (1976); A. J. Millis, *ibid.* **48**, 7183 (1993); T. Moriya and T. Takimoto, J. Phys. Soc. Jpn. **64**, 960 (1995).

[30]S. Watanabe and K. Miyake, J. Phys.: Condens. Matter. **23**, 094217 (2011).

[31]S. Nishiyama, K. Miyake, and C. M. Varma, Phys. Rev. B **88**, 014510 (2013).